CHAPTER - VI

Sorption and Desorption of Rhodamine 6G and Rhodamine B on Na-Laponite System.

In order to investigate further, the influence of the type of clay mineral on ion-exchange behaviour of Na-Laponite XLG, a synthetic hectorite, has been used for the sorption and desorption of RG^+ and RB^+. Although laponite, montmorillonite are members of the expanding three layer clays, the difference among these members is in the type and degree of the isomorphic substitution. Laponite owes its charge to octahedral replacement of Mg^{2+} by Li^+ while in montmorillonite it is primarily Mg^{2+} for Al^{3+} in the octahedral layer (1,2). Consequently the electrical attraction between montmorillonite plate differs greatly from that of laponite as a result of which laponite possesses lower charge density than montmorillonite (3) and can well more freely in aqueous medium.

The properties of this synthetic clay mineral has been described by Fripiat (4) and Neuman et al (5,6). The stability of a laponite CP Sol in presence of Chlorides of lithium, sodium, potassium, ammonium, magnesium calcium, barium, lanthanum and hexadecyltrimethylammonium bromide has been studied over a wide range of pH by Perkins et al (7). They observed that the sols

are stable over the pH range $\approx$ 7-12 and laponite CP particle - charge becomes more negative as the pH increases. At pH $<$ 7, sols are destabilised. Thus laponite CP clay suspension behaves quite differently with regard to the stability towards electrolytes as a function of pH than montmorillonite. Laponite CP is also chosen because it forms stable colloid solutions suitable for spectrophotometric studies. So the present investigation has been carried out with the synthetic laponite XLG, supplied by Laponite Industries Ltd., England.

The sorption and desorption characteristics of RG^+ and RB^+ on Na-laponite are discussed below on the basis of experimental results. The characteristics of sorption are presented in Section A and those of desorption in Section B. In Section A also infrared studies on RG^+ and RB^+ exchanged Na-Laponite are briefly discussed.

SECTION - A

Studies on Sorption

Sorption RG^+ at pH 8.5

The adsorption isotherm of RG^+ on Na-laponite is shown in Fig. 42(a) and the Fig. 42(b) represents linear Langmuir reciprocal graph from which the value of V_m is found to be 96 meq/100 gm as against the amount of dye exchanged at 1.2×10^{-4} (M) which is 92 meq/100g. Both these values are higher than cation exchange capacity of the clay mineral. The top portion of the isotherm has not attained a plateau upto the concentration used in this study. But this nature was not shown in case of montmorillonite (page 59). Since laponite can swell to an unlimited extent, the dye molecules get sufficient space for an easy entry into the interlamellar region and stack themselves upto formation of a bilayer or multilayer. Also the higher aggregation tendency of RG^+ in aqueous medium favours this process (page 61). The Langmuir bonding constant of the dye calculated from the slope and intercept of the linear plot is $2.14 \times 10^5\ M^{-1}$.

Sorption of RB^+ at pH 8.5

The adsorption of RB^+ on Na-laponite is drawn in Fig. 49(a). The plot of C/XVX C, where C is the equilibrium concentration of RB^+ and X is the amount adsorbed per 100 gm of the adsorbent, yields a good straight line Fig. 49(b). This indicates that the sorption data conform to the Langmuir equation suggesting a monolayer adsorption. From the slope of the straight line, the value of V_m (the amount required to form a complete monolayer) is found to be 89 meq/100 gm. The maximum exchange from the adsorption isotherm is 92 meq/100 gm while the c.e.c. of the mineral is 88 meq/100 gm. These values are lower than those for RG^+ but still slightly higher than the c.e.c. value of Na-laponite. This is probably due to sorption of aggregated ions from the solution or dimerisation or stacking of dye ions over those already present in the adsorbed state. Here the value of V_m is less than that of RG^+ adsorbed. This may be due to lower aggregation tendency of RB^+ compared to RG^+ in aqueous medium. The calculated Langmuir constant for RB^+ on to laponite is equal to $2.26 \times 10^5 M^{-1}$. which is higher than that of RG-Na-laponite system, signifying that the former dye is more firmly anchored to the mineral. Similar characteristics of these dyes have been found earlier on montmorillonite and kaolinite.

Infrared Spectral Studies on RG^+ and RB^+ exchanged Na-Laponite.

Following the method given in Chapter - III page 55 infrared spectra are obtained for RG, RB, Na-laponite, 100% RG - exchanged and 100% RB-exchanged laponite shown in Figs. 21, 22, 56, 57, 58 respectively. It appears that the ring vibration band of RG^+ at 1580 cm^{-1} (Fig. 21) has been shifted to 1605 cm^{-1} (Fig. 57) for 100% RG-exchanged Na-laponite. This band of RB at 1602 cm^{-1} (Fig. 22) has been shifted to 1590 cm^{-1} (Fig. 58) for 100% RB-exchanged Na-laponite. Experimental result reflects their behaviour towards aggregation in the interlayer space (8).

SECTION - B

Desorption Studies

Desorption of RG^+ from Na-Laponite - RG:

The results of desorption of RG^+ from Na-laponite-RG complex by inorganic and organic ions are shown in Figs. 43-47. The desorption curves for inorganic and organic ions are similar to those obtained in the case of Na-montmorillonite. From table 10 it can be seen that selectivity coefficients increase in the order $Li^+ < Na^+ < K^+ \leqslant NH_4^+ < Rb^+ < Cs^+$ for the monovalent and $Mg^{++} < Ca^{++} < Sr^{++} < Ba^{++}$ for the bivalent cations. Similarly for the monovalent organic ions used the selectivity coefficients are in the following sequence: $(CH_3)_4N < (C_2H_5)_4N < (C_3H_7)_4N < (C_4H_9)_4N$ and for the organic monovalent long chain surface active ions $DDTMA^+ < DDP^+ < CTMA^+ < CP^+$. The higher exchange ability of NH_4^+ than K^+ is to be noted which has also been observed by Bhattacharyya (9) in the desorption of $diquat^{2+}$ from Na-laponite-diquat complex and by Sunwar (10) in the desorption of $thionine^+$ from Na-laponite-thionine complex. It is interesting to note that the extent of desorption of RG^+ by inorganic monovalent, and bivalent cations (Figs. 43-44) is lower than that observed in montmorillonite. The charge density of the minerals is in the order : Laponite < montmorillonite and so the strength of binding would be the greater with montmorillonite than laponite.

This would lead probably to the expectation that the extent of desorption of the dye will be more in laponite system and lesser in montmorillonite system.

However, nitrogen sorption study shows that the surface area of laponite is larger than that of montmorillonite (11) and so the exchange sites in the former are more widely spaced than in the latter as a result of which the smaller inorganic ions are unable to approach the exchange spots effectively to displace the adsorbed dye from the laponite matrix.

It is also observed that the amount of RG^+ desorbed from Na-laponite-RG complex by $CTMA^+$ or CP^+ is greater than the smaller ions $(CH_3)_4N^+$ or $(C_2H_5)_4N^+$. Since Na-laponite shows considerable interlamellar swelling in an aqueous medium, steric and space factors do not influence the extent of exchange. As such from the observed isotherms (Fig. 45) it reveals that there is a regular increase in the affinity of alkyl ammonium ions for laponite with increasing molecular weight and molecular size. Similar behaviour is found in chain lengths of the long chain surface active ions (Figs. 46, 47). This applies, to the adsorption of organic compounds by expanding clay minerals in general and is ascribed to the increased contribution of van der Waals forces to the adsorption energy (12) and changes in the hydration states of the ions in the clay interlayer (13,14).

As in the desorption of RG^+ from its montmorillonite complexes, both $1/a^o$ and hydrated ionic radius of the alkaline earth metal ions when polotted against log (selectivity coefficient)

behave linearly (Fig. 48). While only $1/a^{o}$ in the case of alkali metal ions yield a straight line when plotted against log (selectivity coefficient) but show non linear when log (selectivity coefficient) plotted against hydrated ionic radii (Fig. 48). Thus the linear relationship of these parameters with log (selectivity coefficient) may be used to correlate and predict the relative affinities of the respective ions for the aluminosilicate surface. As mentioned earlier (page 73) the obedience of the exchange data to the Pauley's model demonstrates that the coulombic interaction between the counter ions and the fixed ionic groups is the predominant factor in this type of exchange reactions.

SECTION - B

Desorption Studies

Desorption of RB^+ from Na-Laponite - RB :

The extent of RB^+ desorbed from Na-laponite-RB complex by various inorganic ions is much smaller than in Na-laponite-RB systems (Figs. 50,51). This is probably due to combined effect of the stronger binding of RB^+ ions onto the mineral reflected from Langmuir bonding constant value and the weak desorbing power of the above ions owing to their relative shape and size vis-a-vis the widely placed exchange sites in laponite interlayer.

In the desorption study with organic ions the percentage of the dye released from Na-laponite-RB complex is lesser than from Na-laponite-RG complex (Figs. 52-54). However, the desorption of the dye increases with the size of the organic ions as in other cases. According to their order of the exchange power, as well as distribution and selectivity coefficients shown in Table 11 the ions may be arranged as $Li^+ < Na^+ < K^+ < NH_4^+ < Rb^+ < Cs^+$ for the monovalent ions, $Mg^{+2} < Ca^{+2} < Sr^{+2} < Ba^{+2}$ for the bivalent ions, in inorganic electrolytes.

According to their exchanging power, the organic ions may be arranged as $TMA^+ < TEA^+ < TPA^+ < TBA^+$ for the tetraalkylammonium ions and $DDTMA^+ < DDP^+ < CTMA^+ < CP^+$ for the monovalent

long chain surface active ions. The exchange isotherm with DDP^+, $DDTMA^+$, $CTMA^+$ and CP^+ are S-shaped and may be explained as done earlier (page 69). Here also CP^+ desorbs a greater amount of dye from $CTMA^+$ due to its lower cmc value. The desorption by $CTMA^+$ and CP^+ at the initial stages is the result of the competition between these electrolytes as single ions and the adsorbed dye ions. But as the concentration of the quarternary salts increases beyond the cmc, the probability of micelle formation increases in the bulk solution and in the adsorbed states. Consequently, the dye ions face a stronger competition and more readily displaced by the quaternary ammonium ions.

As noted in the case of other mineral systems, the extent of desorption of RG^+ from its laponite complex, is higher than that of RB^+ from Na-laponite-RB complex, suggesting thereby a weaker binding to RG^+ to this exchanger. Such order in the binding strengths of RB and RG has also been observed in montmorillonite and kaolinite systems. The higher bonding constant of RB^+ sorption isotherm (page 113) compared to that of RG^+ (page 112) also leads support to this conclusion.

The plot of hydrated ionic radii vs log (slectivity coefficient) though non linear in the case of monovalent inorganic ions, gives a straight line for bivalent inorganic

ions. However, a linear plot is obtained for monovalent and bivalent inorganic ions when their values $1/a^{o}$ are plotted against log (selectivity coefficient) (Fig. 55). A similar behaviour was noted earlier in the other minerals studied.

TABLE - 10

Desorption characteristics of RG from Na-Laponite-RG with respect to different ions

Electrolytes used	Concentration of Electrolyte	Distribution Coefficient	Selectivity Coefficient
1:1 Electrolyte			
LiCl	0.1 (M)	0.029	3.57×10^{-8}
	0.2 (M)	0.022	4.14×10^{-8}
	0.3 (M)	0.018	4.37×10^{-8}
	0.5 (M)	0.014	4.11×10^{-8}
	0.75 (M)	0.010	3.26×10^{-8}
NaCl	0.1 (M)	0.040	6.93×10^{-8}
	0.2 (M)	0.027	6.56×10^{-8}
	0.3 (M)	0.022	6.12×10^{-8}
	0.5 (M)	0.015	5.23×10^{-8}
	0.75 (M)	0.017	4.44×10^{-8}
KCl	0.1 (M)	0.078	2.61×10^{-7}
	0.2 (M)	0.048	2.02×10^{-7}
	0.3 (M)	0.036	1.72×10^{-7}
	0.5 (M)	0.025	1.39×10^{-7}
	0.75 (M)	0.018	1.10×10^{-7}

TABLE - 10 (Contd..)

Electrolytes used	Concentration of Electrolyte	Distribution Coefficient	Selectivity Coefficient
	0.1 (M)	0.063	1.69×10^{-7}
NH_4Cl	0.2 (M)	0.041	1.48×10^{-7}
	0.3 (M)	0.033	1.45×10^{-7}
	0.5 (M)	0.025	1.40×10^{-7}
	0.75 (M)	0.019	1.23×10^{-7}
	0.1 (M)	0.094	3.84×10^{-7}
RbCl	0.2 (M)	0.056	2.77×10^{-7}
	0.3 (M)	0.042	2.28×10^{-7}
	0.5 (M)	0.028	1.75×10^{-7}
	0.75 (M)	0.021	1.50×10^{-7}
	0.1 (M)	0.138	8.32×10^{-7}
CsCl	0.2 (M)	0.082	5.92×10^{-7}
	0.3 (M)	0.061	4.92×10^{-7}
	0.5 (M)	0.041	3.83×10^{-7}
	0.75 (M)	0.029	2.94×10^{-7}

TABLE -10 (Contd..)

Electrolytes used	Concentration of Electrolyte	Distribution Coefficient	Selectivity Coefficient
2:1 Electrolyte			
$MgCl_2$	0.05 (M)	0.449	1.94×10^{-6}
	0.10 (M)	0.327	1.50×10^{-6}
	0.20 (M)	0.236	1.14×10^{-6}
	0.30 (M)	0.196	9.82×10^{-7}
	0.40 (M)	0.172	8.79×10^{-7}
$CaCl_2$	0.05 (M)	0.468	2.21×10^{-6}
	0.10 (M)	0.342	1.73×10^{-6}
	0.20 (M)	0.247	1.30×10^{-6}
	0.30 (M)	0.205	1.13×10^{-6}
	0.40 (M)	0.181	1.02×10^{-6}
$SrCl_2$	0.05 (M)	0.476	2.32×10^{-6}
	0.10 (M)	0.344	1.75×10^{-6}
	0.20 (M)	0.252	1.38×10^{-6}
	0.30 (M)	0.210	1.20×10^{-6}
	0.40 (M)	0.183	1.07×10^{-6}

TABLE - 10 (Contd..)

Electrolytes used	Concentration of Electrolyte	Distribution Coefficient	Selectivity Coefficient
	0.05 (M)	0.526	3.15×10^{-6}
$BaCl_2$	0.10 (M)	0.385	2.48×10^{-6}
	0.20 (M)	0.280	1.91×10^{-6}
	0.30 (M)	0.231	1.62×10^{-6}
	0.40 (M)	0.202	1.44×10^{-6}
Quaternary Ammonium Salt			
	0.05 (M)	0.189	7.67×10^{-7}
TMABr	0.10 (M)	0.151	9.87×10^{-7}
	0.20 (M)	0.104	9.46×10^{-7}
	0.30 (M)	0.075	7.53×10^{-7}
	0.40 (M)	0.066	7.73×10^{-7}
	0.05 (M)	0.415	3.78×10^{-6}
TEABr	0.10 (M)	0.302	4.06×10^{-6}
	0.20 (M)	0.204	3.79×10^{-6}
	0.30 (M)	0.157	3.40×10^{-6}
	0.40 (M)	0.132	3.23×10^{-6}

TABLE - 10 (Contd..)

Electrolytes used	Concentration of Electrolyte	Distribution Coefficient	Selectivity Coefficient
	0.05 (M)	1.739	7.42×10^{-5}
TPABr	0.10 (M)	1.072	5.85×10^{-5}
	0.20 (M)	0.730	5.88×10^{-5}
	0.30 (M)	0.596	6.31×10^{-5}
	0.40 (M)	0.510	6.52×10^{-5}
	0.05 (M)	4.032	5.06×10^{-4}
TBABr	0.10 (M)	2.270	3.40×10^{-4}
	0.20 (M)	1.285	2.36×10^{-4}
	0.30 (M)	0.941	2.03×10^{-4}
	0.40 (M)	0.756	1.86×10^{-4}
	2×10^{-4} (M)	189.94	3.23×10^{-3}
DDTMABr	4×10^{-4} (M)	197.36	7.51×10^{-3}
	6×10^{-4} (M)	151.76	7.42×10^{-3}
	8×10^{-4} (M)	134.04	7.32×10^{-3}
	1×10^{-3} (M)	119.82	7.49×10^{-3}

TABLE -10 (Contd..)

Electrolytes used	Concentration of Electrolyte	Distribution Coefficient	Selectivity Coefficient
	2×10^{-4} (M)	709.10	5.49×10^{-2}
CTMABr	4×10^{-4} (M)	481.57	5.63×10^{-2}
	6×10^{-4} (M)	373.37	5.48×10^{-2}
	8×10^{-4} (M)	295.68	4.73×10^{-2}
	1×10^{-3} (M)	245.94	4.19×10^{-2}
	1×10^{-4} (M)	472.97	1.02×10^{-2}
DDPBr	2×10^{-4} (M)	378.18	1.37×10^{-2}
	3×10^{-4} (M)	294.09	1.27×10^{-2}
	4×10^{-4} (M)	252.63	1.28×10^{-2}
	5×10^{-4} (M)	220.54	1.24×10^{-2}
	1×10^{-4} (M)	1009.00	5.12×10^{-2}
CPBr	2×10^{-4} (M)	866.68	8.76×10^{-2}
	3×10^{-4} (M)	705.85	9.48×10^{-2}
	4×10^{-4} (M)	576.31	8.83×10^{-2}
	5×10^{-4} (M)	492.38	8.39×10^{-2}

TABLE - 11

Desorption characteristics of RB from Na-Laponite-RB with respect to different ions.

Electrolyte used	Concentration of Electrolyte	Distribution Coefficient	Selectivity Coefficient
1:1 Electrolyte			
	0.1 (M)	0.012	9.45×10^{-9}
LiCl	0.2 (M)	0.010	9.92×10^{-9}
	0.3 (M)	0.008	1.56×10^{-8}
	0.5 (M)	0.006	1.33×10^{-8}
	0.75 (M)	0.005	1.21×10^{-8}
	0.1 (M)	0.017	1.85×10^{-8}
NaCl	0.2 (M)	0.013	2.08×10^{-8}
	0.3 (M)	0.010	1.98×10^{-8}
	0.5 (M)	0.007	1.82×10^{-8}
	0.75 (M)	0.005	1.64×10^{-8}
	0.1 (M)	0.037	8.82×10^{-8}
KCl	0.2 (M)	0.023	6.50×10^{-8}
	0.3 (M)	0.017	5.59×10^{-8}
	0.5 (M)	0.012	3.68×10^{-8}
	0.75 (M)	0.008	3.30×10^{-8}

TABLE - 11 (Contd..)

Electrolytes used	Concentration of electrolyte	Distribution Coefficient	Selectivity Coefficient
	0.1 (M)	0.042	1.33×10^{-7}
NH_4Cl	0.2 (M)	0.026	8.79×10^{-8}
	0.3 (M)	0.020	7.31×10^{-8}
	0.5 (M)	0.013	5.66×10^{-8}
	0.75 (M)	0.009	1.87×10^{-8}
	0.1 (M)	0.049	1.48×10^{-7}
RbCl	0.2 (M)	0.029	1.07×10^{-7}
	0.3 (M)	0.021	8.75×10^{-8}
	0.5 (M)	0.014	6.64×10^{-8}
	0.75 (M)	0.010	5.37×10^{-8}
	0.1 (M)	0.055	1.92×10^{-7}
CsCl	0.2 (M)	0.033	1.36×10^{-7}
	0.3 (M)	0.025	1.18×10^{-7}
	0.5 (M)	0.017	9.50×10^{-8}
	0.75 (M)	0.013	7.86×10^{-8}

TABLE - 11 (Contd..)

Electrolytes used	Concentration of electrolyte	Distribution Coefficient	Selectivity Coefficient
2:1 Electrolyte			
$MgCl_2$	0.05 (M)	0.294	7.89×10^{-7}
	0.10 (M)	0.228	7.34×10^{-7}
	0.20 (M)	0.172	6.35×10^{-7}
	0.30 (M)	0.144	5.60×10^{-7}
	0.40 (M)	0.127	5.07×10^{-7}
$CaCl_2$	0.05 (M)	0.316	9.83×10^{-7}
	0.10 (M)	0.241	8.70×10^{-7}
	0.20 (M)	0.179	7.17×10^{-7}
	0.30 (M)	0.150	6.37×10^{-7}
	0.40 (M)	0.132	5.82×10^{-7}
$SrCl_2$	0.05 (M)	0.328	1.09×10^{-6}
	0.10 (M)	0.249	9.56×10^{-7}
	0.20 (M)	0.185	7.91×10^{-7}
	0.30 (M)	0.155	6.99×10^{-7}
	0.40 (M)	0.136	6.37×10^{-7}

TABLE -11 (Contd..)

Electrolytes used	Concentration of electrolyte	Distribution Coefficient	Selectivity Coefficient
	0.05 (M)	0.340	1.21×10^{-6}
$BaCl_2$	0.10 (M)	0.255	1.03×10^{-6}
	0.20 (M)	0.192	8.90×10^{-7}
	0.30 (M)	0.163	8.10×10^{-7}
	0.40 (M)	0.145	7.60×10^{-7}
Quaternary Ammonium Salt			
	0.05 (M)	0.031	2.95×10^{-8}
TMABr	0.10 (M)	0.031	5.92×10^{-8}
	0.20 (M)	0.018	4.26×10^{-8}
	0.30 (M)	0.021	8.75×10^{-8}
	0.40 (M)	0.018	8.58×10^{-8}
	0.05 (M)	0.093	2.67×10^{-7}
TEABr	0.10 (M)	0.062	2.38×10^{-7}
	0.20 (M)	0.054	3.67×10^{-7}
	0.30 (M)	0.049	4.63×10^{-7}
	0.40 (M)	0.054	7.47×10^{-7}

TABLE - 11 (Contd..)

Electrolytes used	Concentration of Electrolyte	Distribution Coefficient	Selectivity Coefficient
	0.05 (M)	0.124	4.76×10^{-7}
TPABr	0.10 (M)	0.124	9.62×10^{-7}
	0.20 (M)	0.107	1.45×10^{-6}
	0.30 (M)	0.117	2.64×10^{-6}
	0.40 (M)	0.123	4.04×10^{-6}
	0.05 (M)	0.077	1.96×10^{-5}
TBABr	0.10 (M)	0.670	3.08×10^{-5}
	0.20 (M)	0.488	3.47×10^{-5}
	0.30 (M)	0.382	3.29×10^{-5}
	0.40 (M)	0.321	3.20×10^{-5}
	2×10^{-4} (M)	93.46	1.09×10^{-3}
DDTMABr	4×10^{-4} (M)	93.23	2.26×10^{-3}
	6×10^{-4} (M)	84.87	2.88×10^{-3}
	8×10^{-4} (M)	85.26	4.00×10^{-3}
	1×10^{-3} (M)	77.57	4.14×10^{-3}

TABLE - 11 (Contd..)

Electrolytes used	Concentration of electrolyte	Distribution Coefficient	Selectivity Coefficient
	2×10^{-4} (M)	341.27	1.60×10^{-2}
CTMABr	4×10^{-4} (M)	310.77	2.95×10^{-2}
	6×10^{-4} (M)	242.87	2.83×10^{-2}
	8×10^{-4} (M)	193.77	2.45×10^{-2}
	1×10^{-3} (M)	158.25	2.05×10^{-2}
	1×10^{-4} (M)	186.18	2.18×10^{-3}
DDPBr	2×10^{-4} (M)	155.07	3.10×10^{-3}
	3×10^{-4} (M)	144.77	4.13×10^{-3}
	4×10^{-4} (M)	108.52	3.68×10^{-3}
	5×10^{-4} (M)	124.29	3.16×10^{-3}
	1×10^{-4} (M)	775.77	4.21×10^{-2}
CPBr	2×10^{-4} (M)	697.84	7.69×10^{-2}
	3×10^{-4} (M)	568.52	8.19×10^{-2}
	4×10^{-4} (M)	488.37	8.53×10^{-2}
	5×10^{-4} (M)	427.88	8.56×10^{-2}

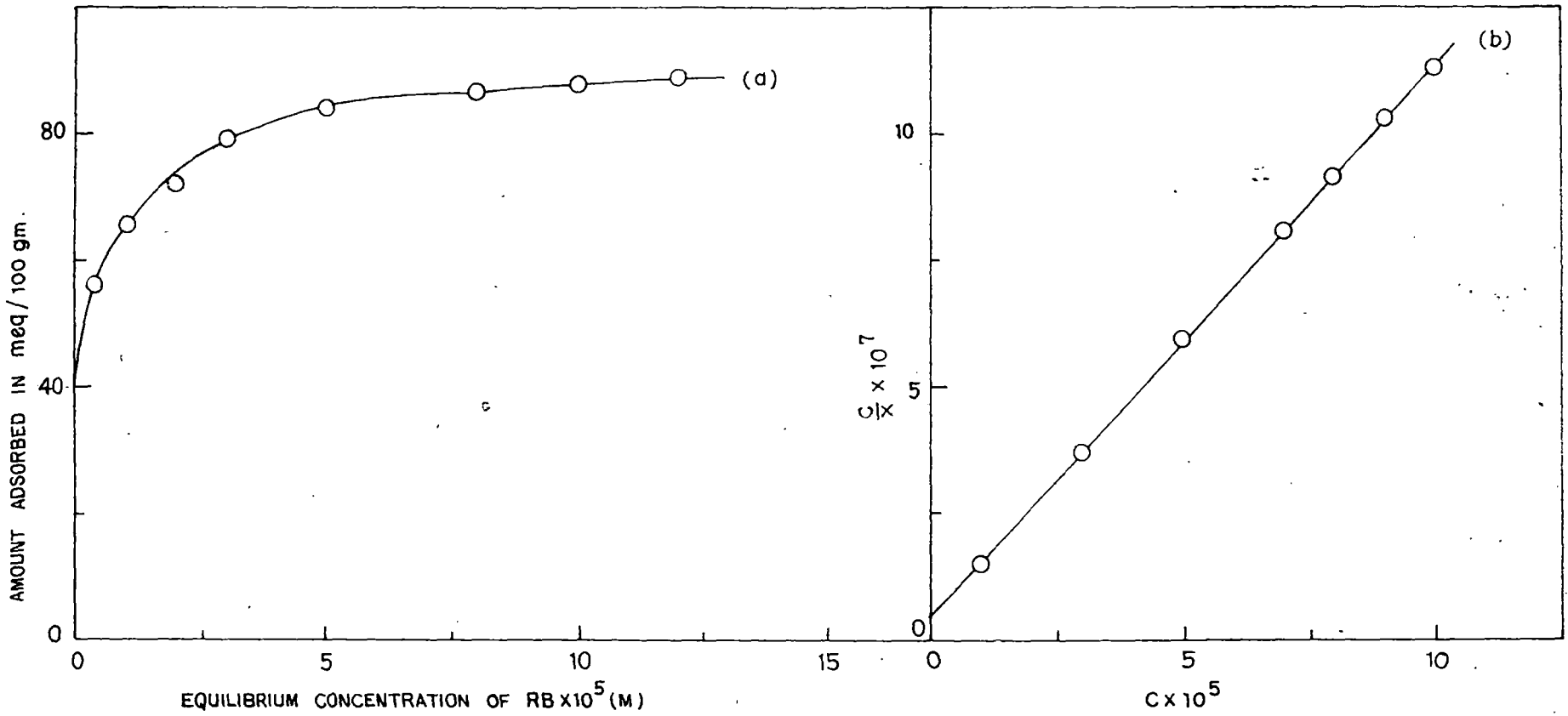

FIG. 42. ADSORPTION ISOTHERM AT 28°C (a) AND LONGMUIR PLOT (b) OF RG ON Na- LAPONITE.

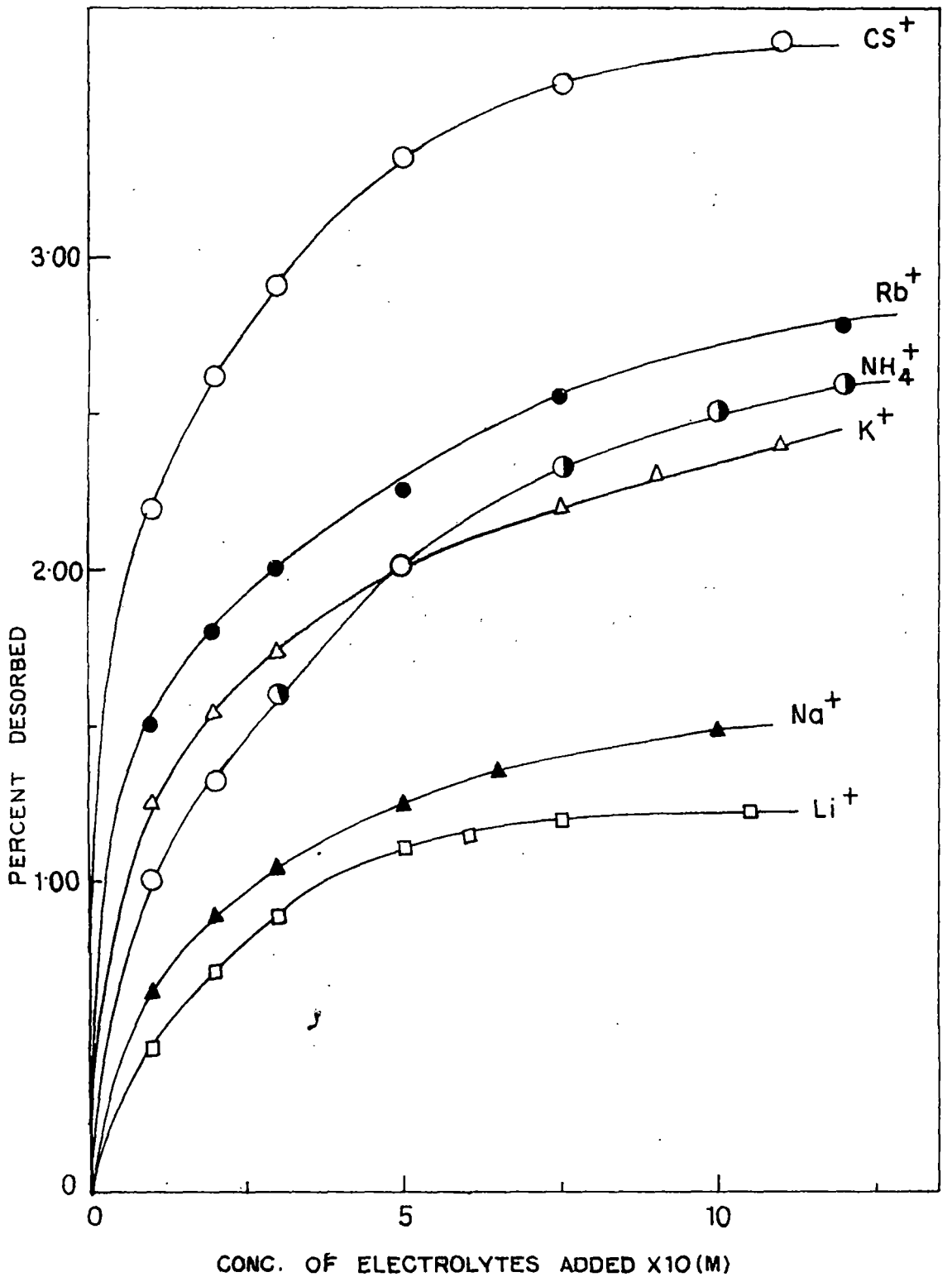

FIG. 43. DESORPTION OF RG FROM Na-LAPONITE-RG BY VARIOUS MONOVALENT IONS.

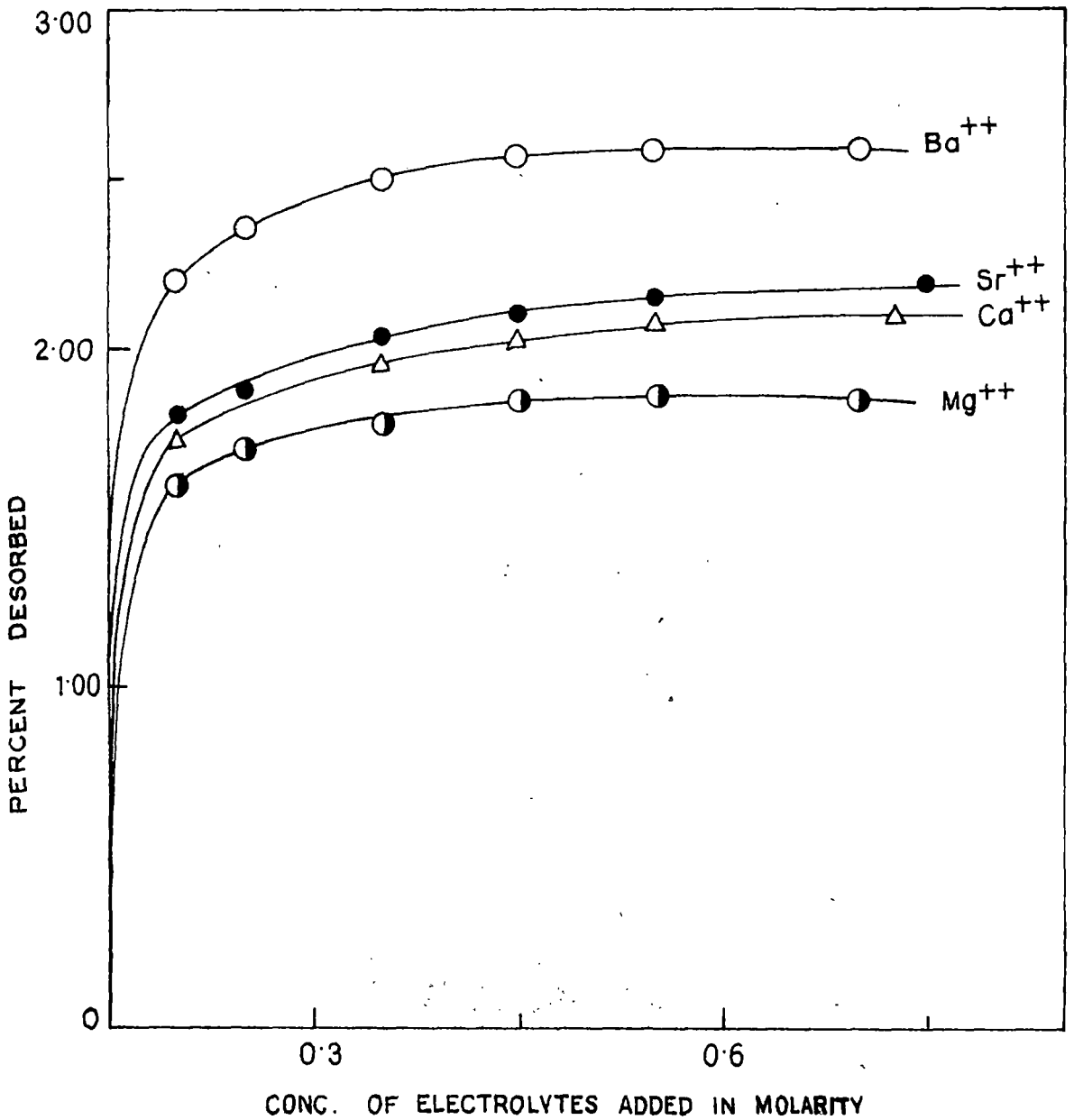

FIG. 44. DESORPTION OF RG FROM Na- LAPONITE - RG BY VARIOUS BIVALENT IONS.

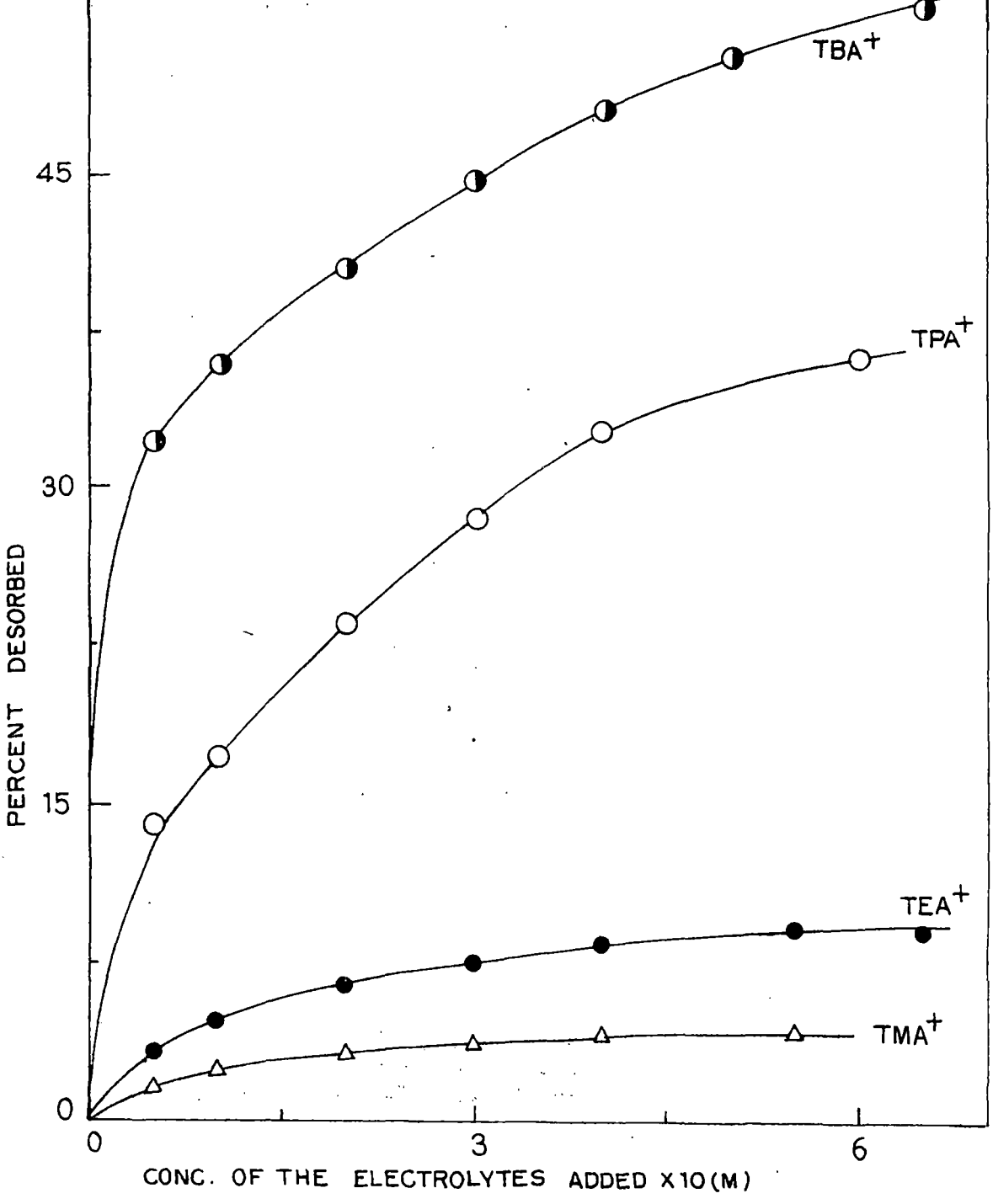

FIG. 45. DESORPTION OF RG FROM Na-LAPONITE-RG BY VARIOUS TETRA ALKYL AMMONIUM HALIDES .

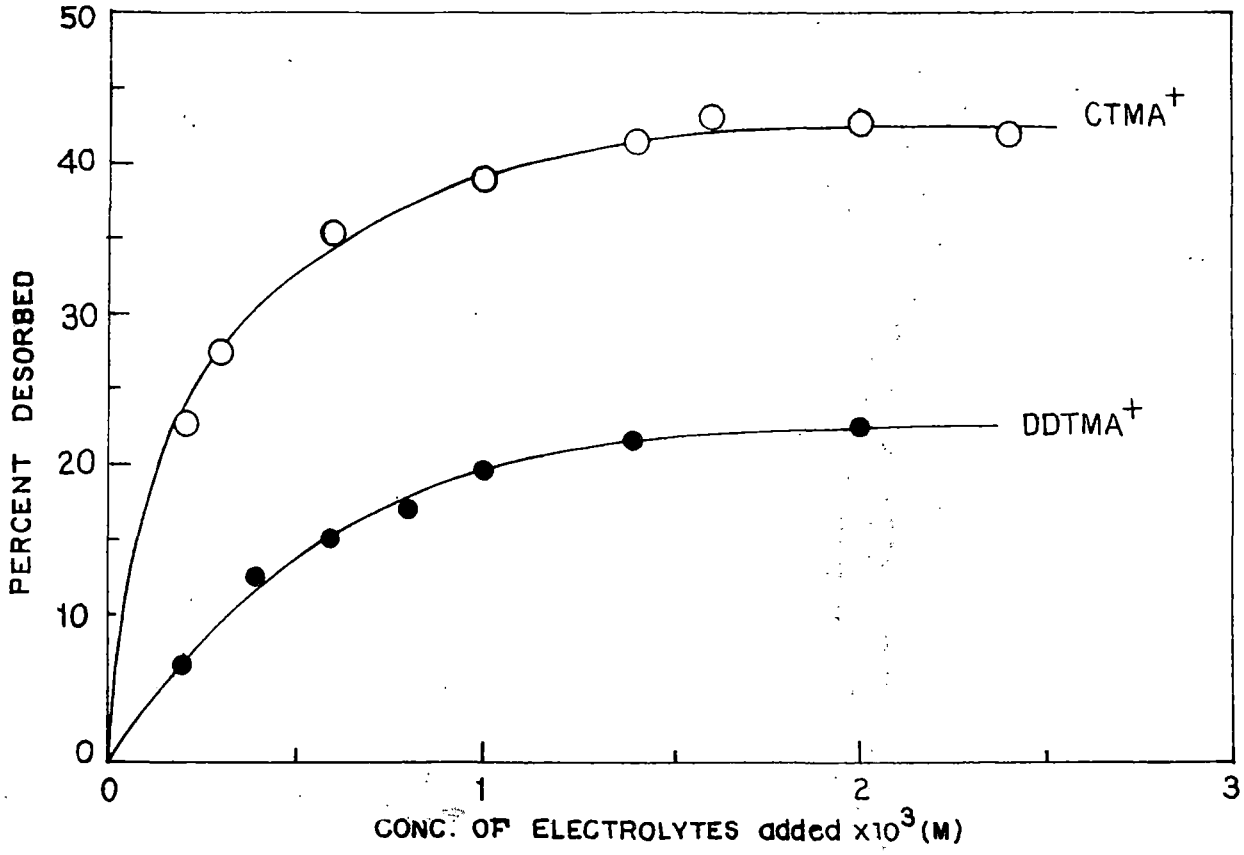

FIG. 46. DESORPTION OF RG FROM Na-LAPONITE-RG BY VARIOUS LONG-CHAIN SURFACE ACTIVE ALKYLTRIMETHYLAMMONIUM HALIDES.

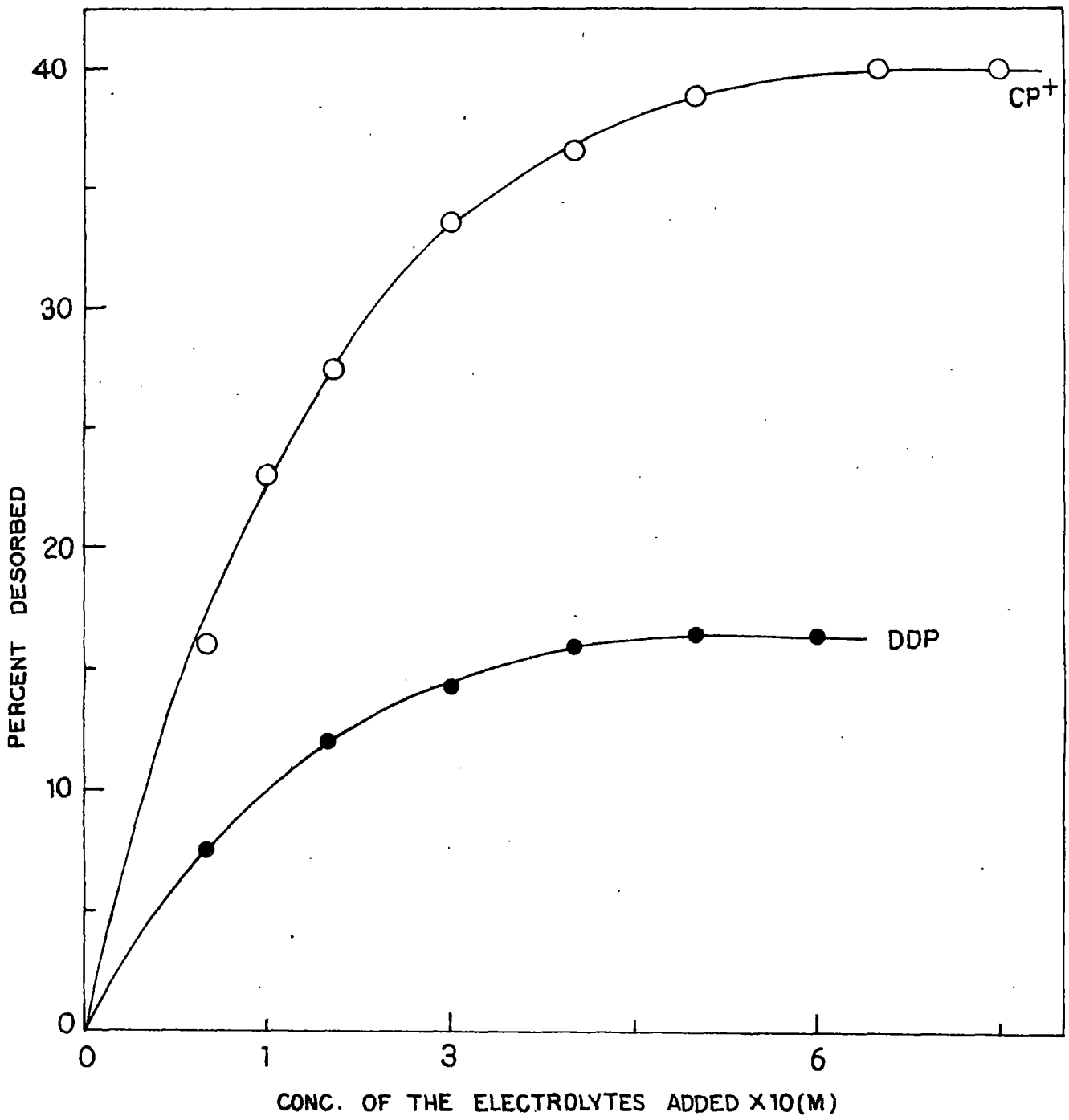

FIG. 47. DESORPTION OF RG FROM Na-LAPONITE-RG BY VARIOUS LONG-CHAIN SURFACE ACTIVE ALKYLPYRIDINIUM HALIDES.

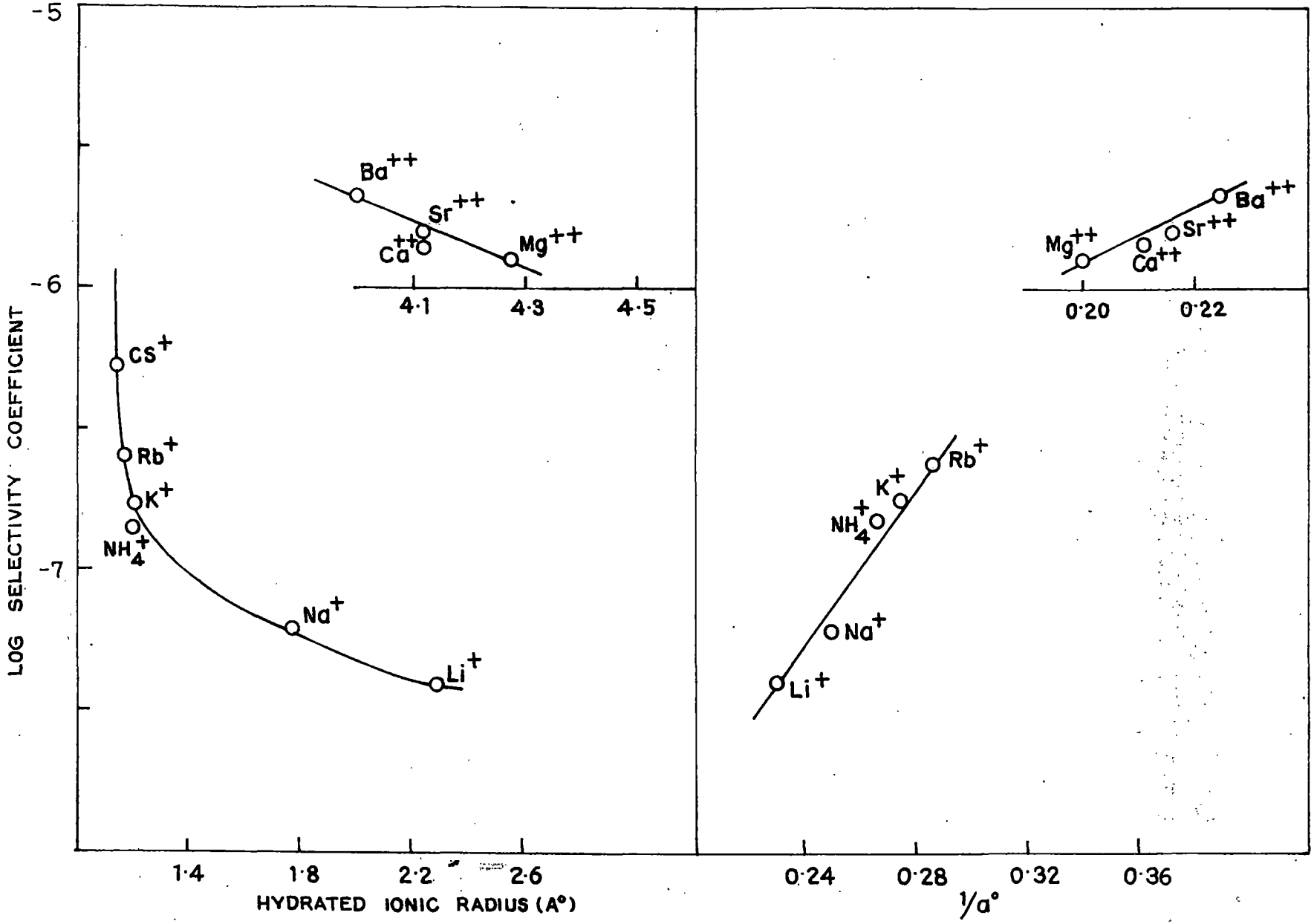

FIG. 48. CORRELATION OF SELECTIVITY COEFFICIENT WITH HYDRATED IONIC RADIUS AND DEBYE-HUCKEL PARAMETER, a°, IN THE DESORPTION OF RG FROM Na - LAPONITE - RG .

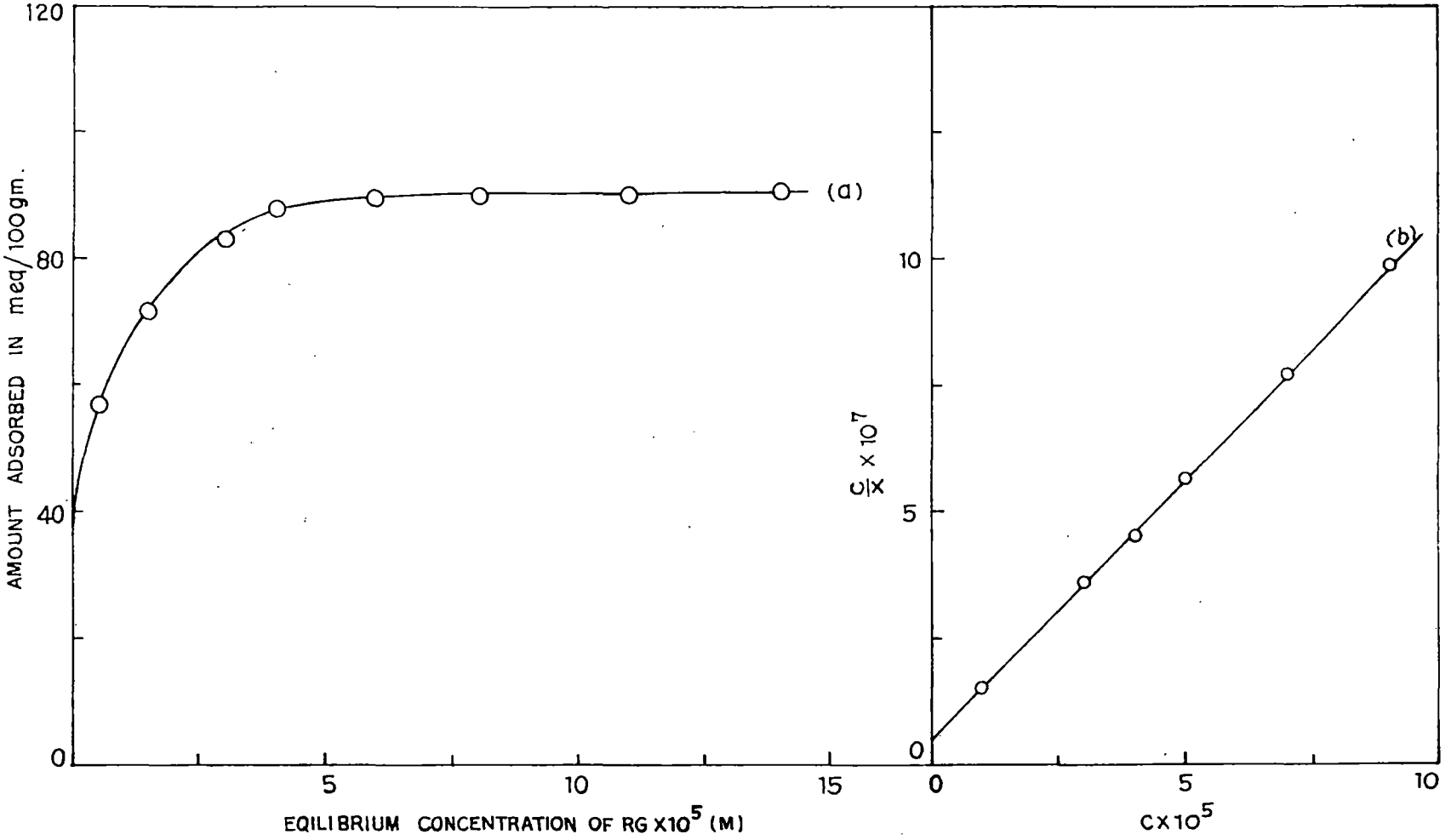

FIG. 49. ADSORPTION ISOTHERMS AT 28°C (a) AND LANGMUIR PLOT (b) OF RB ON Na-LAPONITE .

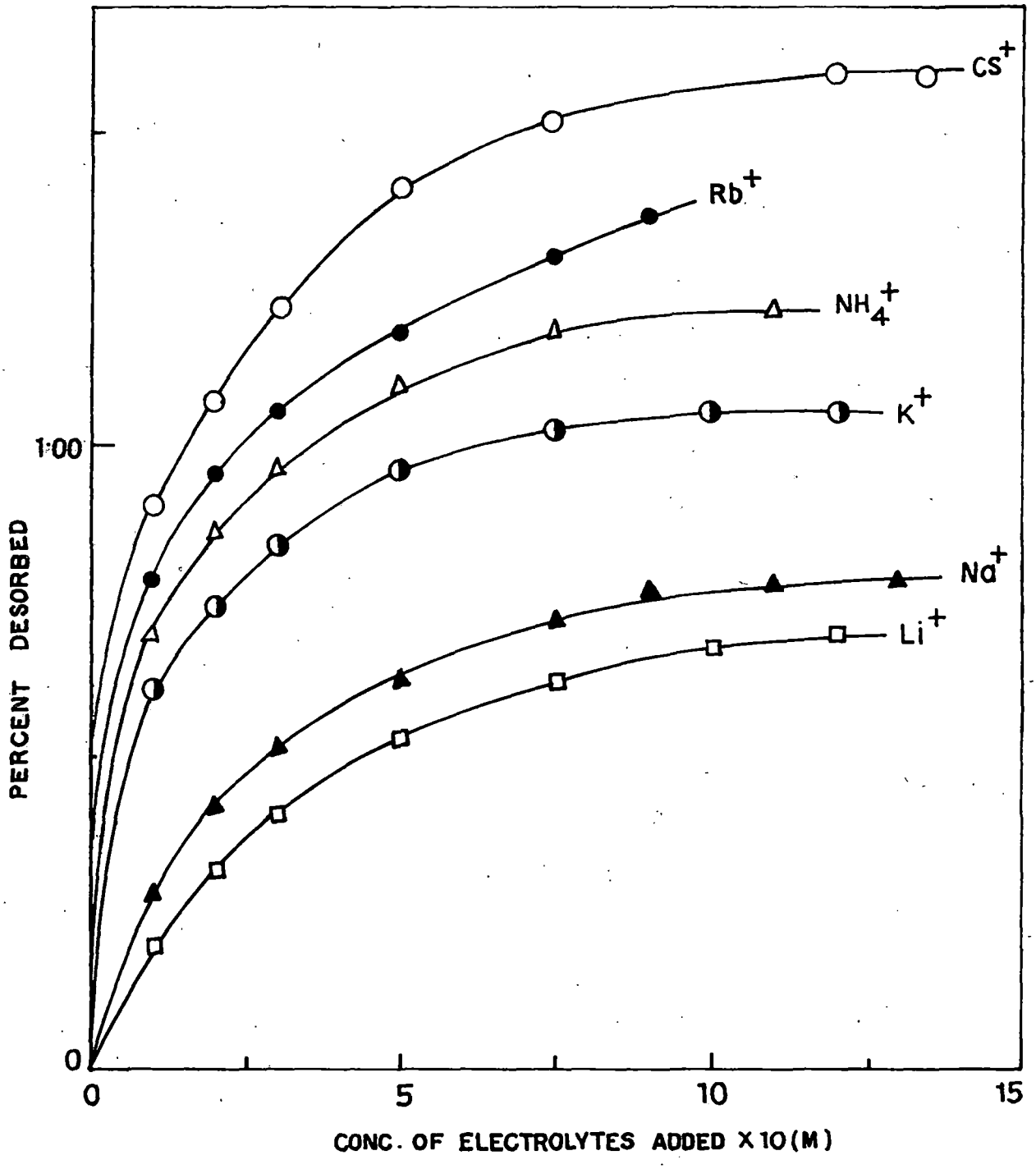

FIG. 50. DESORPTION OF RB FROM Na-LAPONITE-RB BY VARIOUS MONOVALENT IONS.

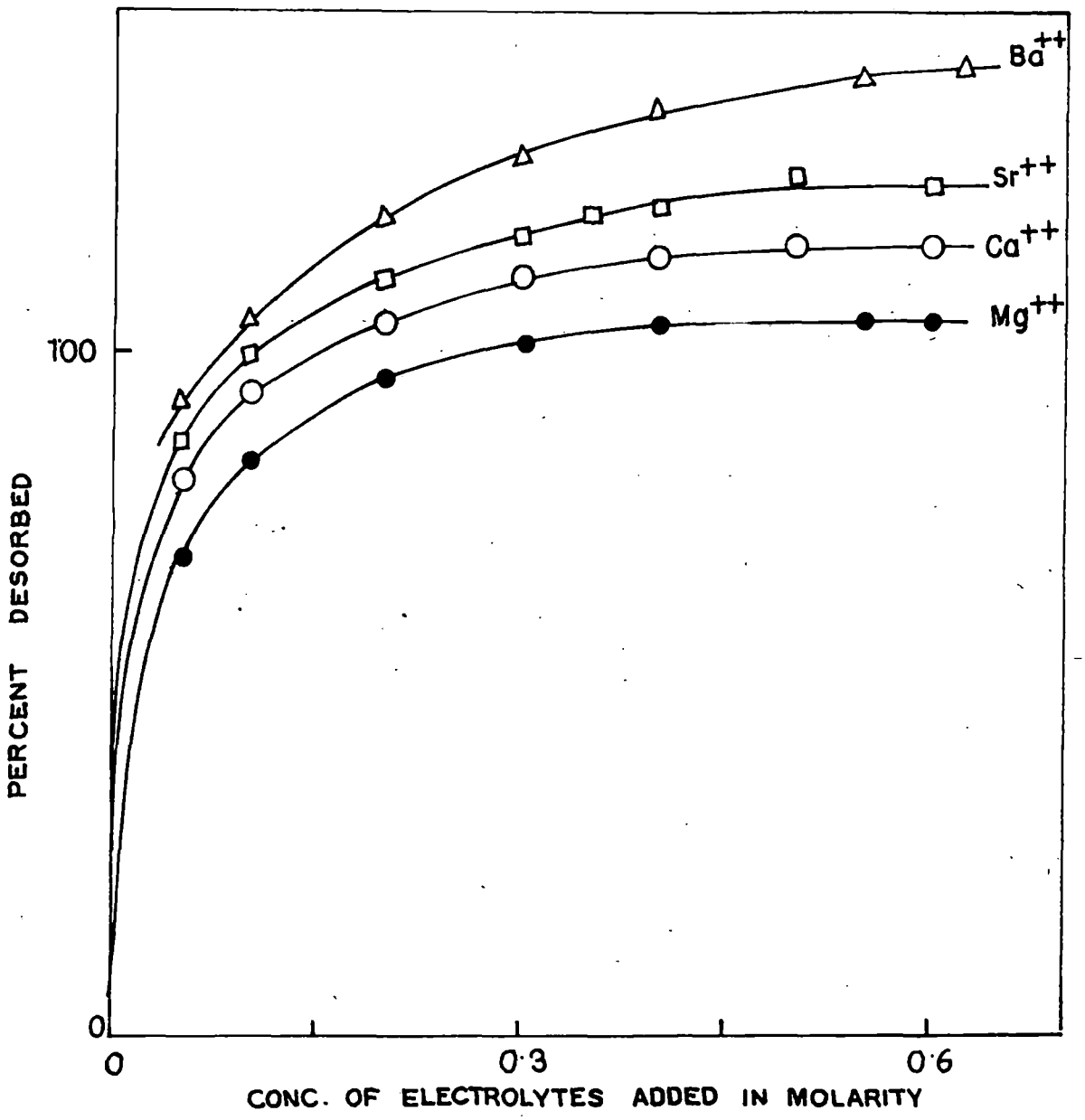

FIG. 51. DESORPTION OF RB FROM Na-LAPONITE-RB BY VARIOUS BIVALENT IONS.

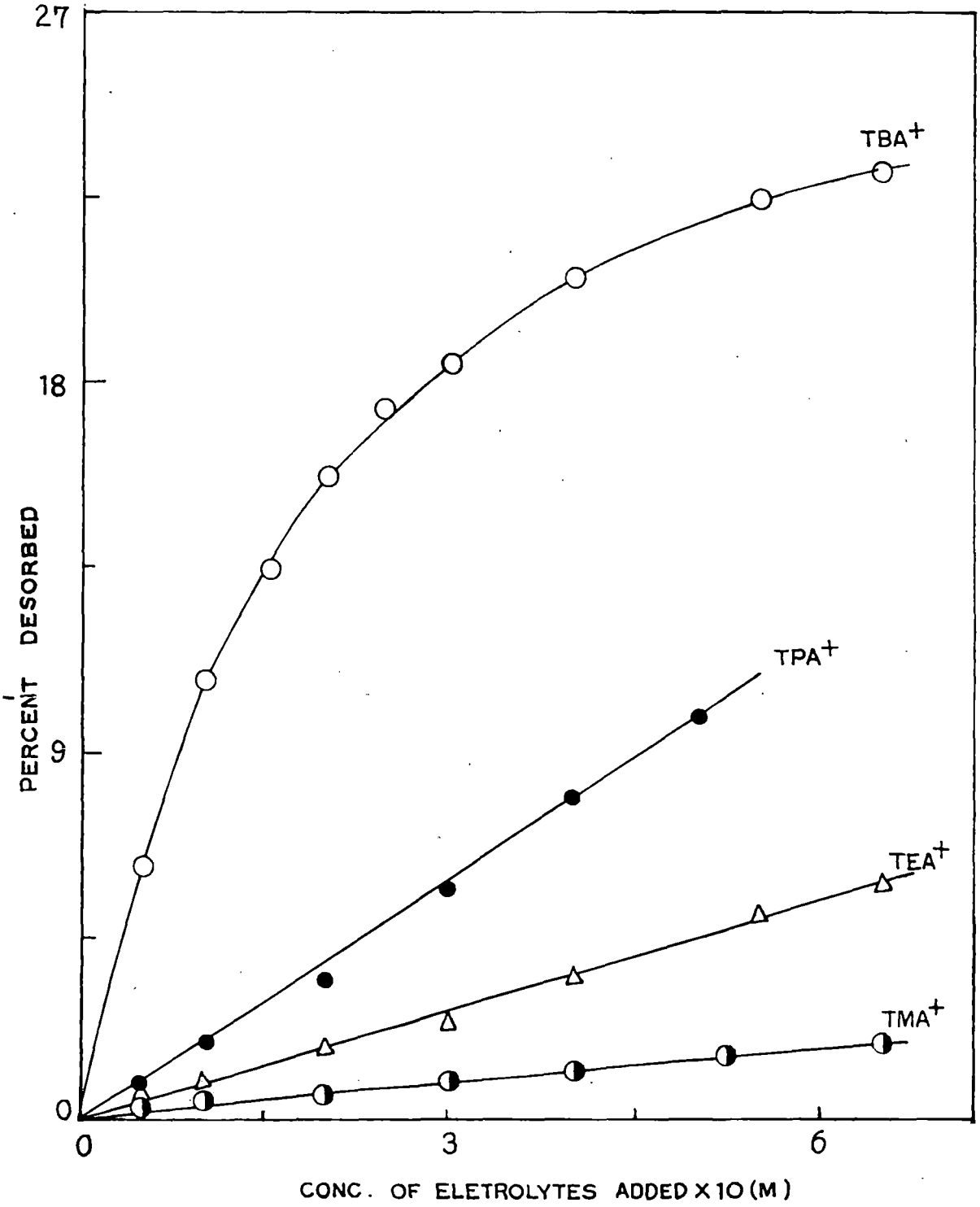

FIG. 52. DESORPTION OF RB FROM Na-LAPONITE-RB BY VARIOUS TETRAALKYLAMMONIUM HALIDES.

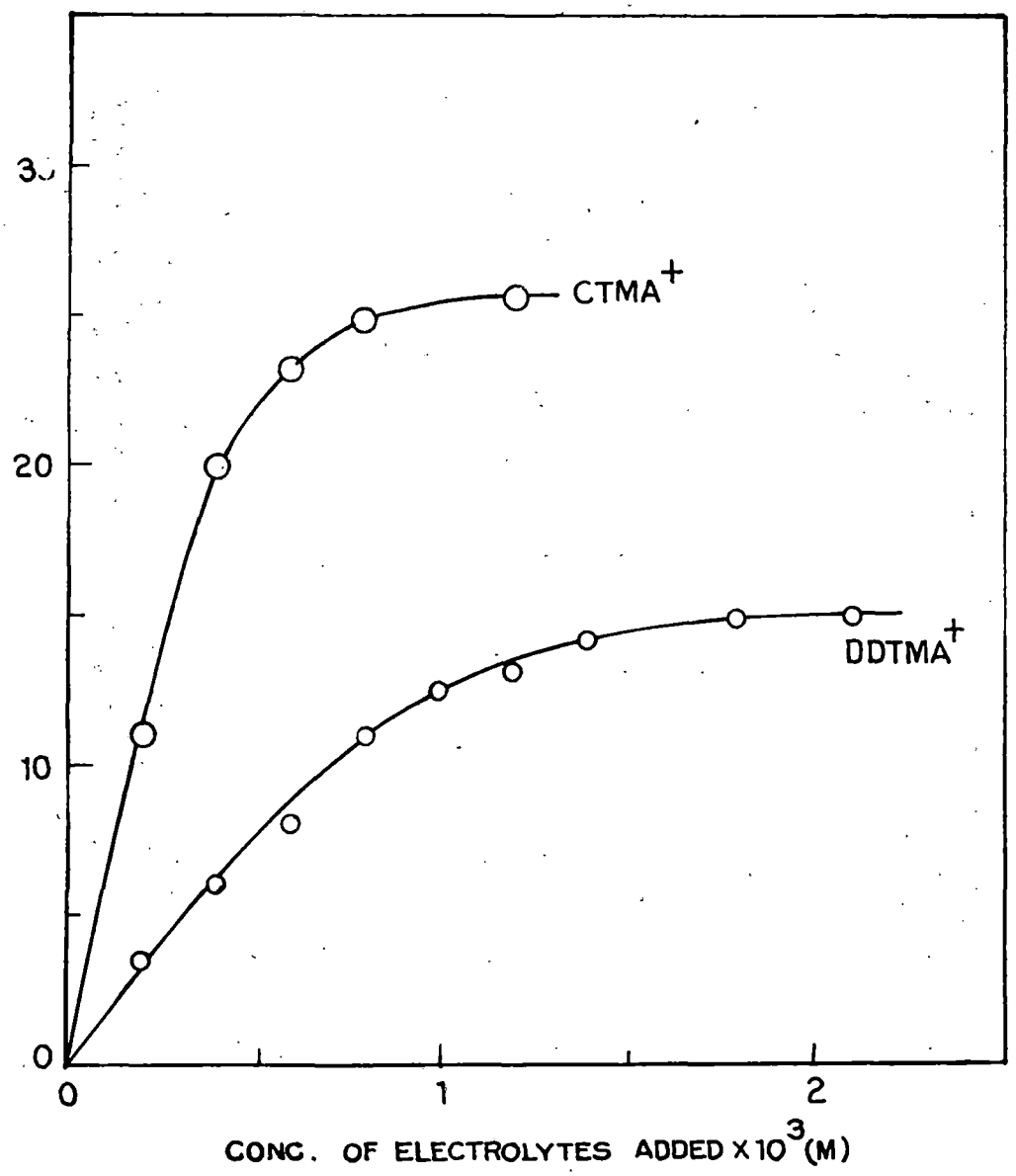

FIG.53. DESORPTION OF RB FROM Na-LAPONITE-RB BY VARIOUS LONG-CHAIN SURFACE ACTIVE ALKYL TRIMETHYL AMMONIUM HALIDES.

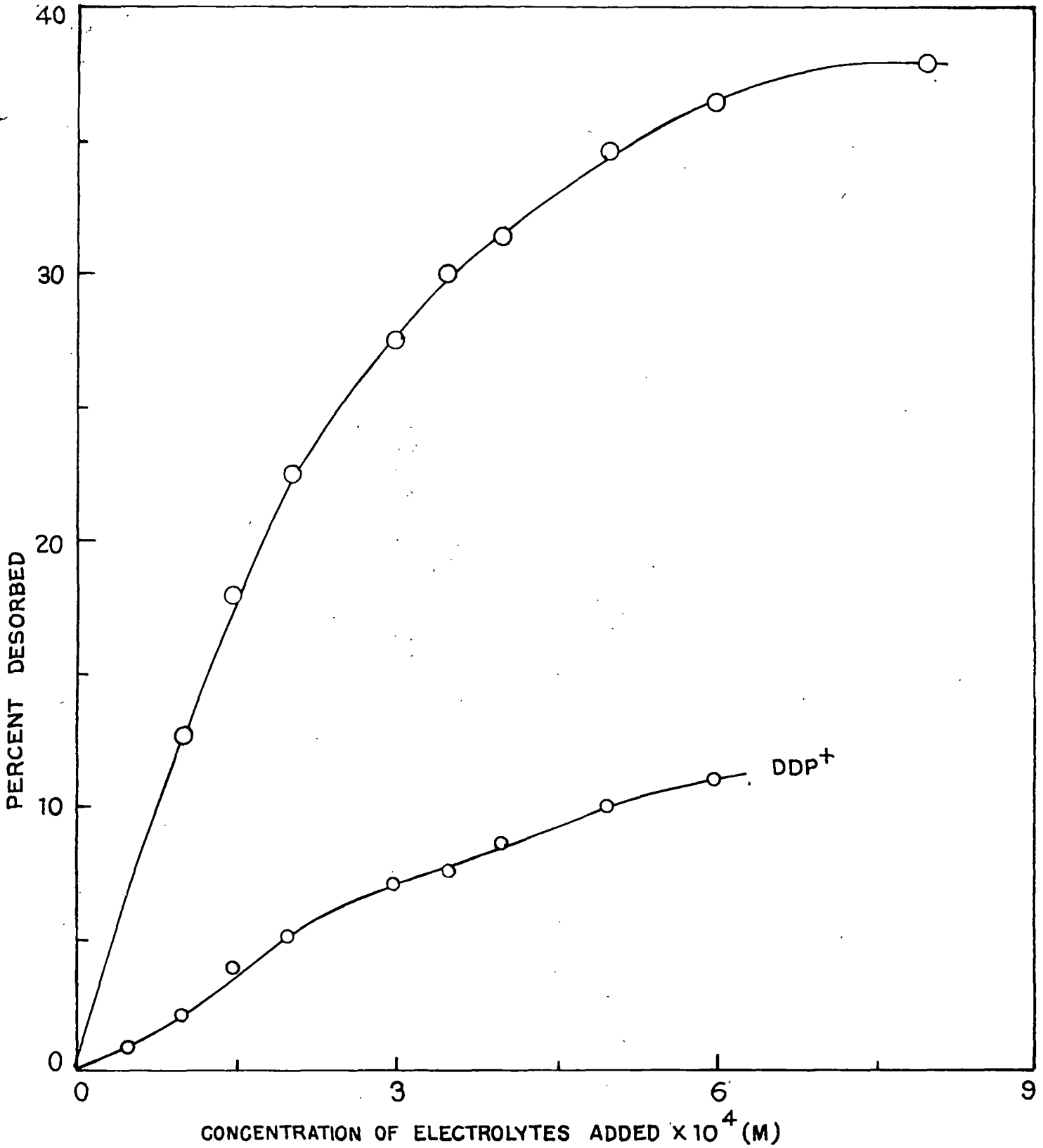

FIG. 54. DESORPTION OF RB FROM Na-LAPONITE-RB BY VARIOUS LONG-CHAIN SURFACE ACTIVE ALKYL PYRIDINIUM HALIDES.

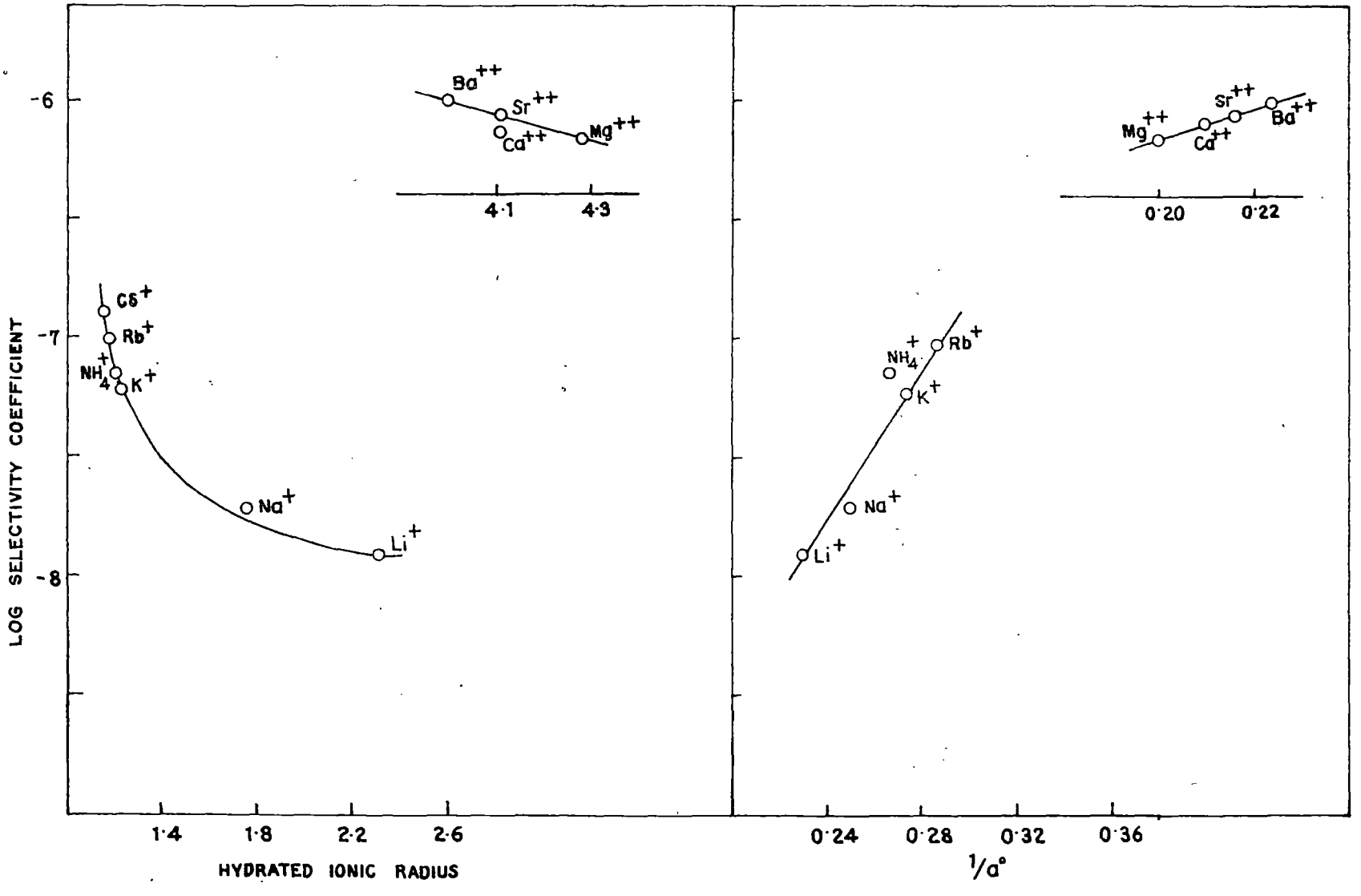

FIG. 55. CORRELATION OF SELECTIVITY COEFFIENT WITH HYDRATED IONIC RADIUS AND DEBYE-HUCKEL PARAMETER, a°, IN THE DESORPTION OF RB FROM Na-LAPONITE-RB.

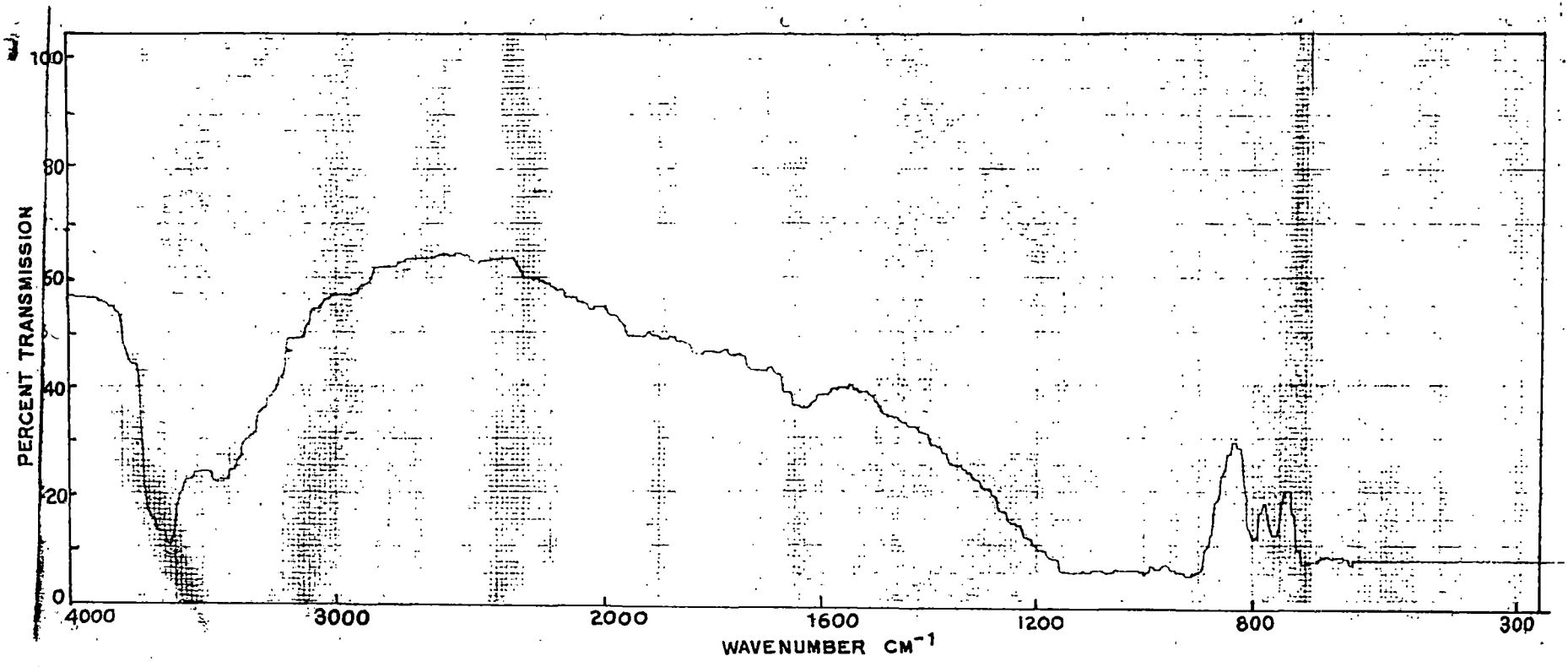

Fig. 56. Infrared Spectrum of Na- Laponite

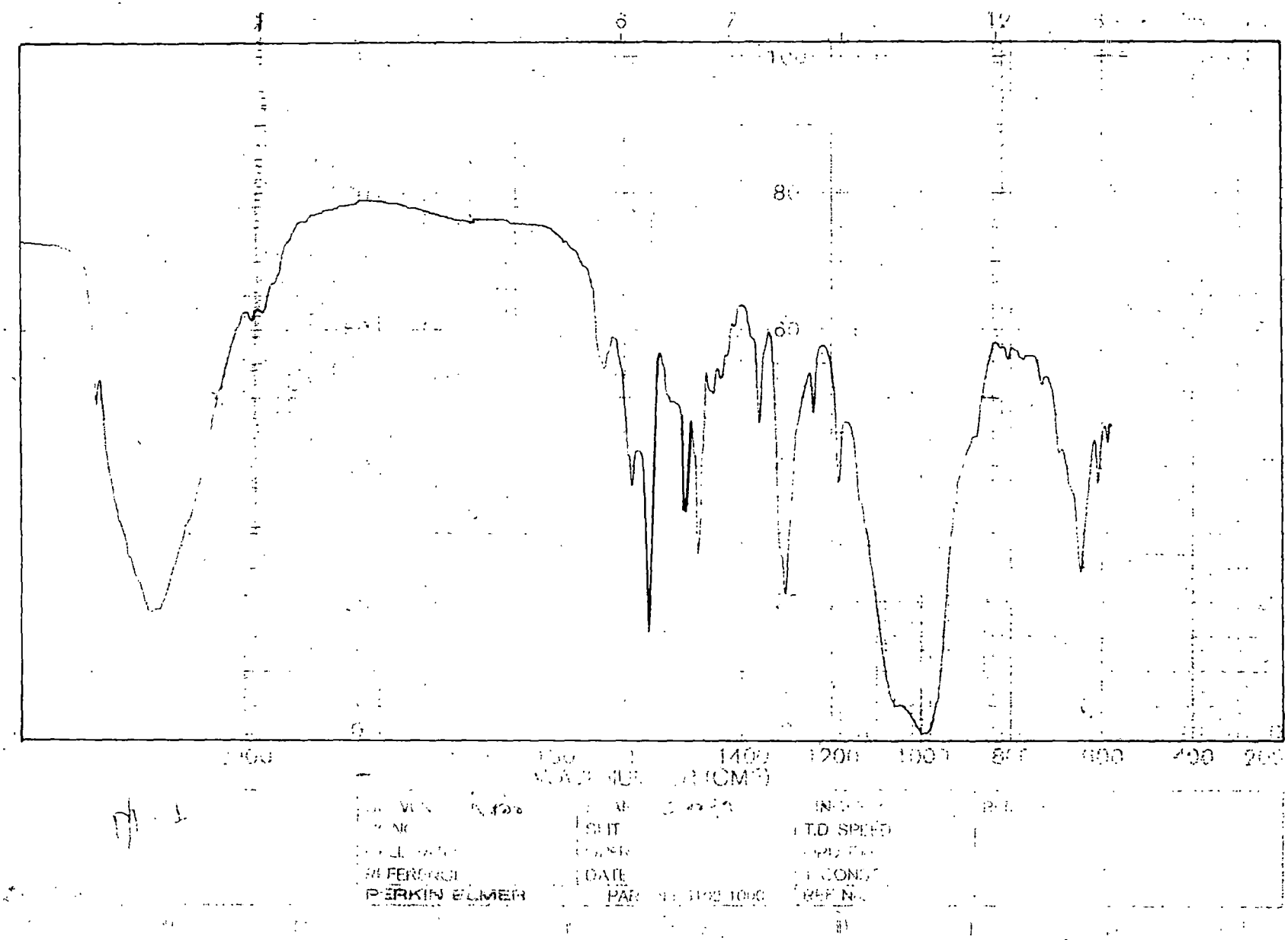

Fig. 57. Infrared spectrum of 100% exchanged Na- Laponite - RG (in KBr pellet).

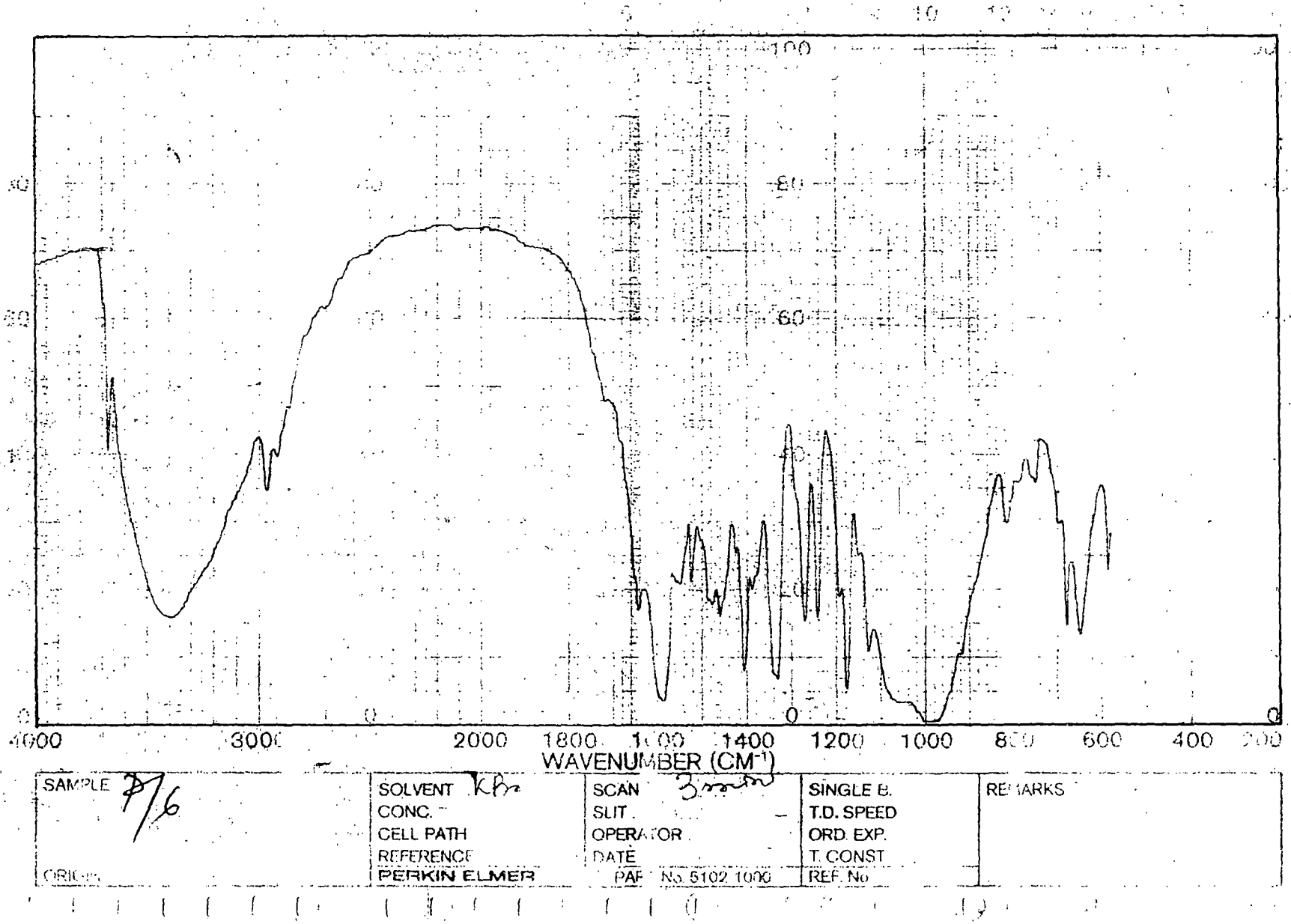

Fig. 58. Infrared spectrum of 100% exchanged Na- Laponite - RB (in KBr pellet)